Journal of Mechanical Engineering Research and Developments
ISSN: 1024-1752
CODEN: JERDFO
Vol. 43, No. 1, pp. 67-75
Published Year 2020

ALE Seamless Immersed Boundary Method with Overset Grid System Adapted to the Shape of an Object

A. Urano*, K. Tajiri1, M. Tanaka, M. Yamakawa & H. Nishida

Department of Mechanophisics, Kyoto Institute of Technology, Hashikami-cho Matsugasaki, Sakyo-Ku, Kyoto 606-8585, Japan

E-mail: m8623005@edu.kit.ac.jp

ABSTRACT: In this study, we constructed the ALE seamless immersed boundary method (ALE SIBM) with the overset grid system using the sub-grid adapted to the shape of an object. In this paper, we discussed the effectiveness of the present method. The ALE SIBM is the combined method of the SIBM and arbitrary Lagrangian-Eulerian (ALE) method to efficiently analyze flow around moving objects on the Cartesian grid. In the ALE SIBM with the overset grid system, the ALE SIBM is applied only to the sub-grid in order to efficiently perform flow analysis including multiple moving objects. Generally, the sub-grid is formed in rectangular area on a Cartesian overset grid. However, depending on the shape of the object, it may form an unnecessary area for flow analysis. Therefore, in this study, in order to reduce unnecessary computational grid points, we constructed the method to reconstruct the sub-grid adapted to the shape of the object. By using the present method, it is possible to compute with the optimal number of the grid points of the sub-grid according to the shape of the object, and the computational cost can be reduced. In this study, ALE-SIBM with the overset grid system adapted to the virtual boundary was applied to the flow including a translating circular cylinder in the channel, and its effectiveness was verified. In order to verify the present method, the results obtained by the present method was compared with the results obtained by the SIBM on the single grid and the conventional ALE-SIBM with the overset grid system non-adapted to the virtual boundary. As a result, the number of computational grid points in the present method was greatly reduced compared to the conventional method. In addition, the results by the present method were in good agreement with the results by other methods quantitatively and qualitatively. Therefore, it was confirmed that the computational accuracy can be maintained while reducing the number of computational grid points by using the present method. In the future, applications to various objects and their verification are desired.

INTRODUCTION

In recent years, the flow phenomenon handled by the computational fluid dynamics become complicated, and the moving boundary problem is handled more and more. Conventionally, the boundary fitted coordinates has been used to analyze flow phenomena around the objects. In this method, computational grid is formed along the shape of the object, and it has high analysis accuracy near the object. However, the computational grid needs to be re-formed when the object moves. This is the problem with boundary fitted coordinates because it is a large computational cost. Therefore, a method using Cartesian coordinate has been proposed in order to make grid reformation unnecessary. In the Cartesian grid approach, the Immersed Boundary Method (IBM) [1] is often adapted because the algorithm is simple. In the IBM, an object is expressed as a set of virtual points, and an additional forcing term that satisfies the velocity conditions on the virtual boundary is added to the governing equations. As for the estimation of the additional forcing term, there are two main methods, that is, the feedback [2,3] and direct [4] forcing term estimations. Generally, the direct forcing term estimation is adopted. However, the conventional IBM with the direct forcing term estimation generates the unphysical pressure oscillations near the virtual boundary because of the pressure jump between inside and outside of the virtual boundary. In order to remove the unphysical pressure oscillations, the seamless IBM (SIBM) [5] was proposed. In the moving boundary problem, whether the IBM or SIBM is used, it is necessary to update the position of the virtual boundary on the computational grid as the object moves. In addition to this, although it is possible to place the fine grid only around the object to improve the computational accuracy, as the movement range of the object is larger, the number of the computational grid points increase. It increases the computational time. In order to solve these problems, a method combining the arbitrary Lagrangian-Eulerian (ALE) method with the SIBM was proposed to perform the computation for the moving boundary problem more efficiency [6]. In the ALE SIBM, since the grid

follows the moving object, it is not necessary to reform the grid and update the position of the virtual boundary. In addition, it is possible to reduce the number of the grid points because the fine grid is formed only near the object. However, since the whole computational grid moves with the object, it has been applied only to a single moving object. Therefore, ALE SIBM on the overset grid was proposed [7]. In the overset grid system, a main-grid is formed throughout the computational domain and sub-grid is formed only around the object. Generally, the boundary fitted grid is used for the sub-grid [8]. However, in this study, the Cartesian grid is used for the sub-grid from the viewpoint of computational efficiency and the SIBM is applied to satisfy the boundary condition. In addition, the ALE method is applied only to the sub-grid, and it follows the moving object. Conventionally, the Cartesian sub-grid was formed in a rectangular area. However, in this case, unnecessary grid points are generated depending on the shape of the object. Therefore, in this study, we propose a method to form the sub-grid in the area according to the shape of the object. By using the present method, it is possible to compute with the optimal number of the grid points of the sub-grid according to the shape of the object, and the computational cost can be reduced. In this study, the effectiveness of the present method is discussed.

ALE SIBM WITH OVERSET GRID SYSTEM

Governing Equation

The governing equations are the continuity equation and the incompressible Navier-Stokes equations based on ALE formulation. In the Navier-Stokes equation based on the ALE formulation, the moving velocity of the computational grid is considered in the advective term. And the forcing term is added to the Navier-Stokes equation for the SIBM. The non-dimensional continuity equation and incompressible Navier-Stokes equations are written as,

$$\frac{\partial u_i}{\partial x_i} = 0, \tag{1}$$

$$\frac{\partial u_i}{\partial t} = F_i - \frac{\partial p}{\partial x_i} + G_i, \tag{2}$$

where, $u_i = (u, v)$, and p are the velocity components and the pressure. And, G_i in the momentum equations denotes the additional forcing term for the SIBM. F_i denotes the convective and diffusion terms.

$$F_i = -(u_j - c_j)\frac{\partial u_i}{\partial x_j} + \frac{1}{Re}\frac{\partial^2 u_i}{\partial x_j \partial x_j}. \tag{3}$$

Where, Re denotes the Reynolds number defined by $Re = L_0 U_0 / \nu_0$. U_0, $L_0$and ν_0 are the reference velocity, the reference length and the kinematic viscosity, respectively. And, c_j is the moving velocity component of the computational grid for the ALE method. In this study, $c_j = 0$ at the main-grid because the ALE method is only applied to the sub-grid.

Numerical Method

The incompressible Navier-Stokes equation is solved by the second order finite difference method on the collocated grid arrangement. The convective, diffusion, and pressure terms are discretized by the conventional second order centered finite difference method. The time derivative terms are discretized by the forward Euler method. For the time integration of the Navier-Stokes equations, the fractional step approach [9] based on the forward Euler method is applied. For the incompressible Navier-Stokes equations in the SIBM, the fractional step approach can be written by

$$u_i^* = u_i^n + \Delta t\, F_i^n, \tag{4}$$

$$u_i^{n+1} = u_i^* + \Delta t \left(-\frac{\partial p^n}{\partial x_i} + G_i^n \right), \tag{5}$$

where u_i^* denotes the fractional step velocity and Δt is the time increment. The resulting pressure equation is

solved by the SOR method.

Seamless Immersed Boundary Method

In order to apply the SIBM, it is necessary to estimate the additional forcing term G_i. In this study, the direct forcing term estimation is adopted in accordance with the previous studies. The direct forcing term estimation in the conventional IBM and SIBM is shown in Fig.1. In the figure, I, J are the grid index. For the forward Euler time integration, the forcing term can be determined by

$$G_i^n = -F_i^n + \frac{\partial p^n}{\partial x_i} + \frac{\bar{U}_i^{n+1} - u_i^n}{\Delta t}, \qquad (6)$$

where $\bar{U}_i^{n+1}$ denotes the velocity linearly interpolated from the velocity on the near grid point and the velocity (u_{vb}) determined by the velocity condition on the virtual boundary. Namely, the forcing term is estimated as the velocity components at next time step satisfy the relation, $u_i^{n+1} = \bar{U}_i^{n+1}$. In the conventional IBM, the forcing term is added only on the grid points near the virtual boundary (show Fig.1 (a)). In this method, the non-negligible velocity appears inside the virtual boundary. Also, the pressure distributions near the virtual boundary show the unphysical oscillations because of the pressure jump. In the SIBM, the forcing term is added not only on the grid points near the virtual boundary but also in the region inside the virtual boundary shown in Fig.1 (b) in order to remove the unphysical oscillations near the virtual boundary. In the region inside the boundary, the forcing term is determined by satisfying the relation, $\bar{U}_i^{n+1} = \bar{U}_b$, where $\bar{U}_b$ is the velocity which satisfies the velocity condition at the grid point [10-13].

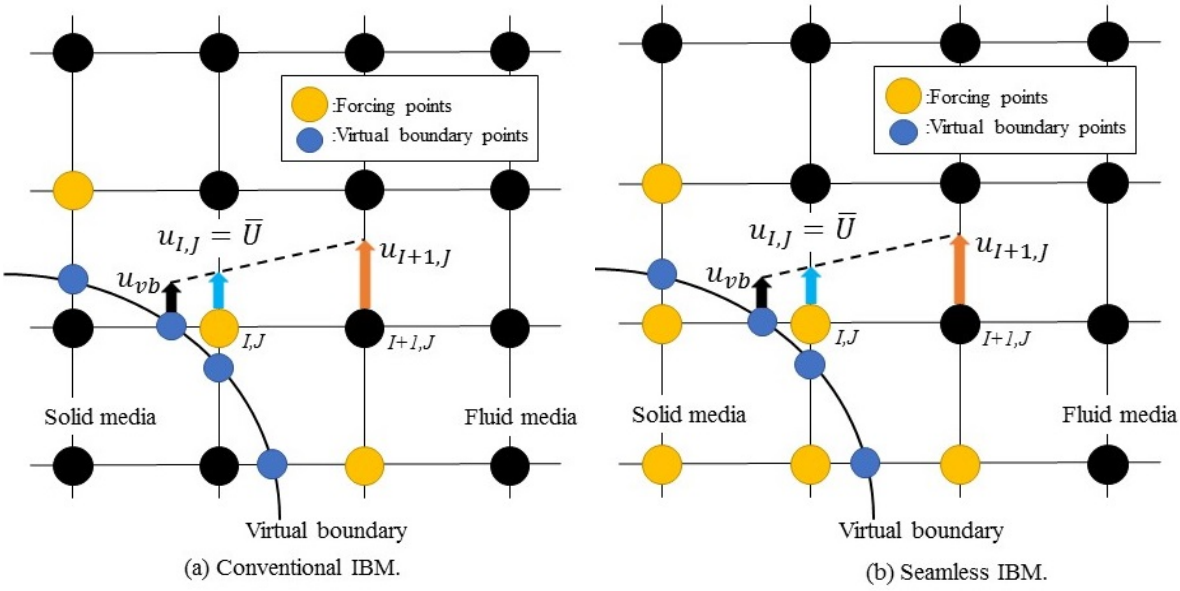

Figure 1. Grid points added forcing term

ALE Method with Overset Grid System

In this study, the overset grid system is used to apply the ALE SIBM to flow including a moving object. In order to solve the governing equations on the overset grid, the main-grid is formed over the entire area, and the sub-grid that follows the movement of the object is formed around the object. And, both the main-grid and the sub-grid are the Cartesian grid. In this method, the position of the object does not change on the sub-grid since the grid follows the movement of the object. In this study, ALE SIBM is applied only to the sub-grid. In the present method, on the main-grid, the quantity values in the region overlapping the sub-grid are interpolated from the sub-grid. In addition, the quantity values at the boundary cell on the sub-grid are similarly interpolated from the main-grid.

Sub-grid Adapted to Virtual Boundary

This section describes how to form the sub-grid adapted to the virtual boundary of the object. First, the conventional rectangular sub-grid is formed around the object. And, on the sub-grid, the only grid points within a certain range from the virtual boundary are used in the analysis. The cells at the edge of the effective sub-grid area are the boundary cell. The quantity values at the boundary cell on the effective sub-grid are similarly interpolated from the main-grid. On the main-grid, the quantity values in the region overlapping the effective sub-grid are interpolated from the sub-grid. Figure 2 shows an example of the sub-grid adapted to the virtual boundary of the circular cylinder. As a result, the computational cost can be reduced because the flow analysis is performed only in the area adapted to the virtual boundary of the object.

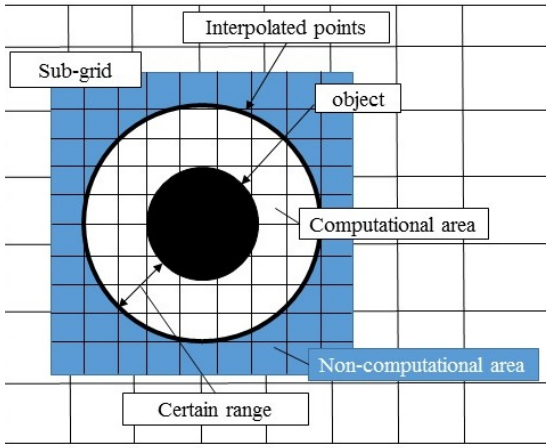

Figure 2. Effective sub-grid area for circular cylinder

APPLICATION TO 2D TRANSLATING CIRCULAR CYLINDER

In order to validate the present method, analysis of the flow around a translating circular cylinder in the channel is performed. The flow analysis under the same conditions are performed on the single grid system and the conventional overset grid system, and are compared with the present method.

Computational Domain and Computational grid

The computational domain is as shown in Fig.3.

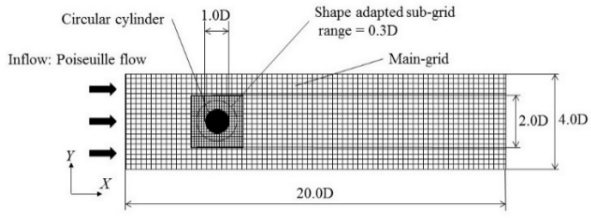

Figure 3. Computational domain

In this study, the computational conditions are classified into four cases according to the type of computational grid and the grid resolution. Case 1 and 2 use overset grids, and cases 3 and 4 use single grids. In cases 1 and 2 where the overset grid is used, the grid resolutions of the main-grid and sub-grid are the same respectively. In case1, the sub-grid adapted to the virtual boundary is formed, and in case 2 a conventional rectangular sub-grid is formed. In case 3 and 4, different grid resolution is set for each. Table 1 shows the grid resolution in each case.

Table 1. Grid resolution in each case.

	Main-grid	Sub-grid
Case 1	0.025	0.0125
Case 2	0.025	0.0125
Case 3	0.025	

Case 4	0.0125	

The translating circular cylinder is expressed using the SIBM, and its diameter is *D*. And, the coordinates of the center of its initial position is $(4D, 2D)$. The velocity at which this cylinder translates is $u = 0.2\sin(2\pi t)$, and the integral value of the velocity is defined as the position of the cylinder, and the analysis is performed. The sub-grid adapted to the virtual boundary for case 1 is shown in Fig.4.

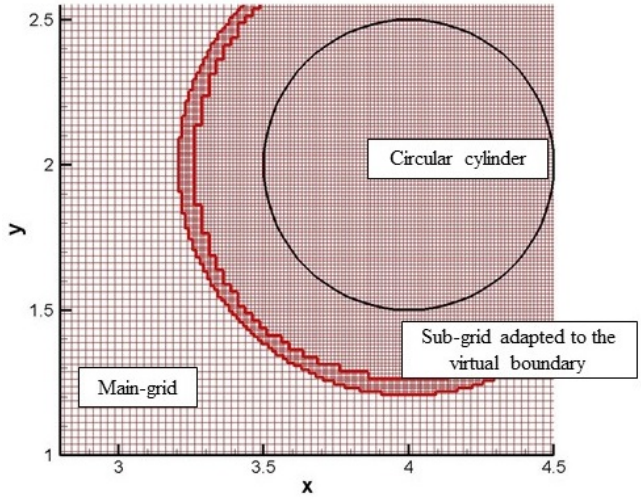

Figure 4. Computational grid near the circular cylinder for case 1

The effective sub-grid area in case 1 is from the virtual boundary to $0.3D$ distance. In this study, since the object is a circular cylinder, the shape of the sub-grid adapted to the virtual boundary is also circular. In case 2, the conventional rectangular sub-grid is used and it has a side of 1.6D. Therefore, the range from the cylinder outer edge to the sub-grid outer edge is $0.3D$, which is the same as in case 1. Table 2 shows the number of computational grid points in each case. Note that the computational grid point is only grid point used to solve the governing equations. In other words, the ineffective sub-grid is not the computational grid point. And, in the overset grid, the grid points in the region overlapping the effective sub-grid is not a computational grid point. From table 2, the number of computational grid points of case 1 and 2 using the overset grid is greatly reduced from case 4, which has the same grid resolution near the cylinder. The number of computational grid points of sub-grid in case 1 is approximately 49% of the number of computational grid points of sub-grid in case 2. The total number of computational grid points (both the main-grid and the sub-grid) does not change much between Case 1 and 2 because the main-grid is relatively fine in this study. If the main-grid is a coarser grid and is formed in a wide domain, it can be expected that the total number of computational grid points is greatly reduced by the reduction of the number of computational grid points of the sub-grid.

Table 2. Number of computational grid points

	Number of computational grid points
Case 1	138232(main:125340 sub:12892)
Case 2	147844(main:121600 sub:26244)
Case 3	128000(800×160)
Case 4	512000(1600×320)

Boundary Conditions

Initial condition is impulsive start where upper and lower walls and a cylinder appear in a two-dimensional Poiseuille flow. For the inflow boundary, the Poiseuille flow is fixed and the pressure is zero-order extrapolation. For the outflow boundary, the velocity is linear extrapolation and the pressure is the Sommerfeld radiation condition. For the upper and lower walls, the velocity is non-slip condition, and the pressure is Neumann condition. At the virtual boundary, the velocity is non-slip condition. Also, the virtual boundary and its inside move to chase the moving cylinder. Reynolds number, time interval are given as follows.

$$Re = 40, \Delta t = 0.001. \quad (7)$$

RESULTS AND DISCUSSIONS

Figures 5,6 show pressure contours in case 1 and 2. In the figures, the solid line shows the outer edge of the cylinder, and the dashed line shows the outer edge of the sub-grid. In case 1, the sub-grid adapted to the virtual boundary is formed, and in case 2 a conventional rectangular sub-grid is formed. The cylinder moves in parallel in the x-direction. The cylinder has a maximum velocity in the positive x-direction at dimensionless time $t = 39.25$ and a maximum velocity in the negative x-direction at $t = 39.75$. The results for these two conditions are shown in the figures. In both results, almost equivalent results are obtained, and the variation of pressure due to the translating of the cylinder is observed. In addition, the smooth pressure distribution is observed near the virtual boundary of the cylinder and at the boundary of the sub-grid.

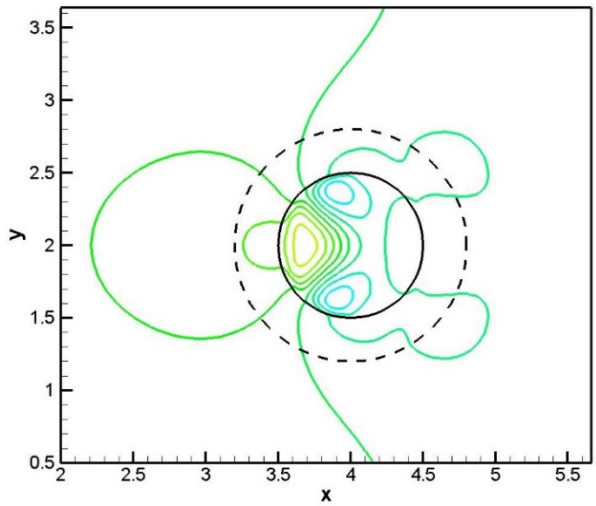

(a) t = 39.25

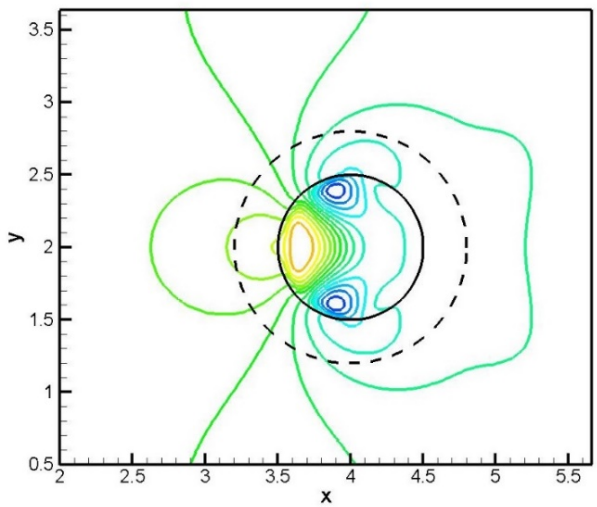

(b) t = 39.75

Figure 5. Close-up view of pressure contours [case 1]

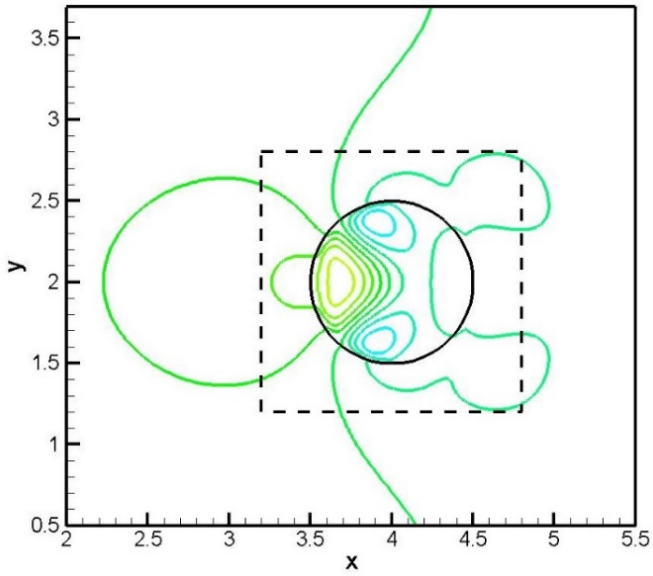

(a) t = 39.25

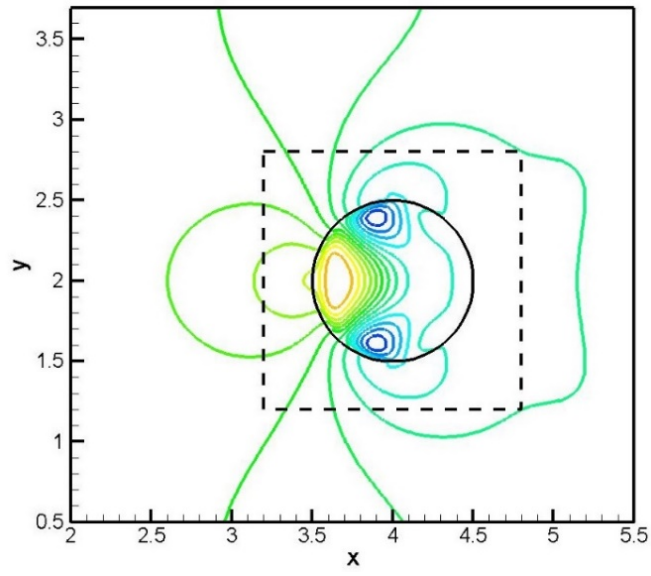

(b) t = 39.75

Figure 6. Close-up view of pressure contours [case 2]

In addition, for quantitative comparison, the drag coefficient is calculated using the following equation.

$$C_D = \frac{-\int_O \left(G_x - u_i \frac{\partial u}{\partial x_i} - \frac{\partial u}{\partial t}\right) ds}{\frac{1}{2}\rho_0 U_0^2 D}. \qquad (8)$$

Where, O indicates the region to which forcing term is applied in the SIBM (see Fig.1). And, ρ_0 is the reference density, and D is the diameter of the cylinder. Figure 9 shows the drag coefficient obtained by each case in the dimensionless time range $t = 30$ to 34. From this figure, it is shown that the drag coefficients of each cases in good agreement. There is a slight vibration in case 3 of the single grid which resolution is 0.025, however, the results of the cases1 and 2, which adopt the overset grid system, show the smooth curves like the case 4 of the single grid which resolution is 0.0125. From these quantitatively and qualitatively comparison of the results of cases 1,2 and 4, the results of the overset grid system are in good agreement with the results of the single grid with

fine resolution. Therefore, the effectiveness of the overset grid system was confirmed. And more, the results of the case 1 which adopt the present method uses the sub-grid adapted to the virtual boundary of the object shows the good agreement with the results of the case 2 which uses the conventional rectangular sub-grid. Therefore, the validity of the present method was confirmed.

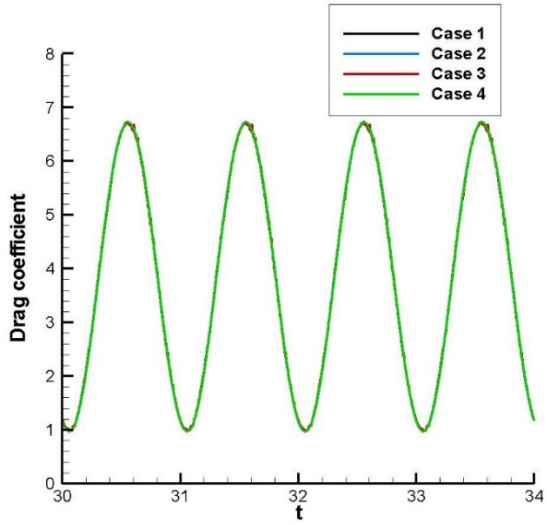

Figure 9. Time history of drag coefficient

CONCLUSION

In this study, ALE-SIBM with the overset grid system adapted to the virtual boundary was applied to the flow including a translating circular cylinder in the channel, and its effectiveness was verified. In order to verify the present method, the results obtained by the present method was compared with the results obtained by the SIBM on the single grid and the conventional ALE-SIBM with the overset grid system non-adapted to the virtual boundary. The number of computational grid points in the present method was greatly reduced compared to the conventional method. In addition, the results by the present method were in good agreement with the results by other methods quantitatively and qualitatively. Therefore, it was confirmed that the computational accuracy can be maintained while reducing the number of computational grid points by using the present method. In the future, applications to various objects and their verification are desired.

NOMENCLATURE

p non-dimensional pressure
t non-dimensional time
c_i convective velocity
u_i non-dimensional velocity component
x_i non-dimensional Cartesian coordinate
C_D drag coefficient
C_L lift coefficient
D reference length of flow around a circular cylinder, m
G_i additional forcing term
Re Reynolds number
U reference velocity, m/s
ν kinematic viscosity, m^2/s
ρ reference density, kg/m^3
Δt time increment

REFERENCES

[1] C.S. Peskin, D.M. McQueen. “A three-dimensional computational method for blood flow in the heart I. immersed elastic fibers in a viscous incompressible fluid”. *Journal of Computational Physics*, Vol. 81, no. 2, pp. 372–405, 1989.

[2] D. Goldstein, R. Handler, L. Sirovich. “Modeling a No-Slip Flow Boundary with an External Force Field”. *Journal of Computational Physics*, Vol. 105, no. 2, pp. 354–366, 1993.

[3] E. M. Saiki, S. Biringen. “Numerical Simulation of a Cylinder in Uniform Flow: Application of a Virtual Boundary Method”. *Journal of Computational Physics*, Vol, 123, no. 2, pp. 450–465, 1996.

[4] A. Zada, S. Ali. “Stability Analysis of Periodic and Almost-Periodic Discrete Switched Linear System”. *Matrix Science Mathematic*, vol. 2, no. 2, pp. 01-06, 2018.

[5] M. Elmnifi, M. Amhamed, N. Abdelwanis, O. Imrayed. “Solar Supported Steam Production for Power Generation in Libya. *Acta Mechanica Malaysia*, vol. 2, no. 2, pp. 05-09, 2018.

[6] K.S.N.H. Ku Mohd Razali, S. Kasim, R. Hassan, H.N. Mahdin, A.A. Ramli, M.F. Md Fudzee, M.A. Salamat. “Lensalyza Photography Studio Reservation System”. *Acta Electronica Malaysia*, vol. 2, no. 2, pp. 06-09, 2018.

[7] R. Kumar. “Comparison of Instruction Scheduling and Register Allocation for Mips And Hpl -Pd Architecture for Exploitation of Instruction Level Parallelism”. *Engineering Heritage Journal*, vol. 2, no. 2, pp. 04-08, 2018.

[8] E. A. Fadlun, R. Verzicco, P. Orlandi, J. Mohd-Yosof. “Combined immersed-boundary finite-difference methods for three-dimensional complex simulations”. *Journal of Computational Physics*, Vol.161, no. 1, pp. 35–60, 2000.

[9] H. Nishida, K. Sasao. “Incompressible Flow Simulations Using Virtual Boundary Method with New Direct Forcing Terms Estimation”. *Proceedings of International Conference on Computational Fluid Dynamics* 2006, pp. 185–186, 2006.

[10] K. Tajiri, H. Nishida, M. Tanaka. “Large Eddy Simulation of Turbulent Flow using Seamless Immersed Boundary Method”. *Proceedings of 8th International Conference on Computational Fluid Dynamics*, Vol. 0197, pp. 1–13, 2014.

[11] K. Tajiri, H. Nishida, M. Tanaka. “ALE Seamless Immersed Boundary Method with Overset Grid System for Multiple Moving Objects”. *Proceedings of 10th International Conference on Computational Fluid Dynamics*, Vol. 047, pp. 1–13, 2018.

[12] J. A. Benek, P. G. Buning, J. L. Steger. “A 3-D chimera grid embedding technique”. *AIAA Paper*, pp. 85-1523, 1985.

[13] C. M. Rhie, W. L. Chow. “Numerical Study of the Turbulent Flow Past an Airfoil with Trailing Edge Separation”. *AIAA journal*, Vol. 21, no. 11, pp. 1525-1532, 1983.